RESEARCH ARTICLE
SPECIAL FOCUS: ONCOLOGY

Carrier-based intralymphatic cisplatin chemotherapy for the treatment of metastatic squamous cell carcinoma of the head & neck

Background: Since head and neck squamous cell carcinoma (HNSCC) preferentially metastasizes to the locoregional lymphatics, treatment of the tumor-draining cervical lymph nodes is paramount. **Results:** We developed a hyaluronan–cisplatin (HA–Pt) nanoconjugate with prolonged lymphatic retention and greatly improved tumor tissue deposition for the treatment of metastatic HNSCC. We also developed an orthotopic metastatic xenograft model of HNSCC to examine the efficacy of the nanoconjugate. HNSCC (1/week × 3 weeks) were completely cured for 57% of the female mice in the HA–Pt treatment group, which demonstrated greatly hindered HNSCC progression compared with the standard cisplatin therapy ($p < 0.05$). **Conclusion:** With this insight, we will be able to optimize the carriers for better uptake, penetration and retention within cancer cells.

Shuang Cai[1], Yumei Xie[2], Neal M Davies[3], Mark S Cohen[4] & M Laird Forrest[†1]

[1]Department of Pharmaceutical Chemistry, University of Kansas, Lawrence, KS 66047, USA
[2]The Pacific Northwest National Laboratory, Richland, WA 99354, USA
[3]Washington State University, Pullman, WA 99164, USA
[4]University of Kansas Medical Center, Kansas City, KS 66160, USA
[†]Author for correspondence:
Tel.: +1 785 864 4388
Fax: +1 785 864 5736
E-mail: mforrest@ku.edu

Head and neck carcinoma is the sixth most common cancer worldwide, encompassing epithelial carcinomas and squamous cell carcinomas characterized by their pathological characteristics [1]. Cancer in the head and neck region can arise from soft tissues, bones and a variety of glands in the upper aerodigestive tracts, including the oral cavity, oropharynx, hypopharynx, larynx, nasopharynx, paranasal sinuses and salivary glands [2]. Approximately 60,000 Americans are diagnosed with head and neck cancer each year. It has been noted, according to statistics, that the largest of all these is **head and neck squamous cell carcinoma** (HNSCC), where malignancies originate in the most superficial layer of tissues or organs in the head and neck region. Early-stage (stage I and II) local HNSCC has good disease prognosis and local tumor control, yielding a stable survival rate of approximately 81% in the past decade. By contrast, patients with regional or metastatic disease have a poor survival rate (as low as 52 and 26%, respectively) and this has improved little in the past 20 years [1]. Late-stage (stage III or IV) patients are usually diagnosed with multiple lymph nodes disease involvement or distant **metastasis**. In most cases, the patients have to receive neck dissection to examine the area of tumor lymphatic drainage and excise the diseased cervical lymph nodes in the lymphatic basin, preventing further disease recurrence.

Historically, patients with unresectable HNSCC have been treated with radiation therapy. Unfortunately, the 5-year survival was unsatisfactory and disease recurrence usually occurred within 2 years after the radiation therapy. For HNSCC patients, there was an imperative need for a more effective and less invasive regimen after the ablation of the primary tumor. Therefore, concurrent chemoradiotherapy has been readily accepted as a neoadjuvant, as well as an adjuvant therapy for better local and regional control of the disease. Platinum-based **chemotherapy** administered concomitant with radiation therapy has now become the first-line therapeutic strategy in the clinic due to the radiosensitizing property and cytotoxic efficacy of **cisplatin** (CDDP) [3]. Several Phase III clinical trials in locally advanced HNSCC exhibited promising results for CDDP, taxane and 5-fluorouracil three-drug chemotherapy in improving overall survival, particularly for patients with unresectable tumors [4]. However, some clinical trials with CDDP and 5-fluorouracil combination adjuvant chemotherapy followed by radiotherapy showed only minimal improvement in the disease-free survival and locoregional control in comparison with patients who received radiation therapy alone [3]. In addition, most chemotherapeutics, including CDDP, have poor penetration to the lymphatic basin due to its anatomy and monodirectional flow, which limits their efficacy in treating late-stage patients. Herein, we sought to investigate the feasibility of developing a lymphatic drug-delivery system to maximize the efficacy and long-term survival rate of CDDP-based chemotherapy in treating

FUTURE SCIENCE part of fsg

Key Terms

Head and neck squamous cell cancer: Cancer that originates from the mucosal cells that line the surface of the upper aerodigestive tract.

Lymphatic metastasis: Spread of cancer from an organ or tissue to the lymphatic system.

Cancer chemotherapy: Treatment regimen that is administered to destroy cancer cells using cytotoxic drugs.

Cisplatin: Platinum-based chemotherapeutic for the treatment of a wide spectrum of solid tumors, including head and neck squamous cell cancer and ovarian cancer.

Hyaluronan nanocarrier: Nanosized drug-delivery vehicles that is made of anionic, biocompatible, and biodegradable polysaccharide hyaluronan.

locally advanced HNSCC and to reduce its dosing frequency and the associated length of patient hospital stay.

Experimental

■ Materials

Hyaluronan (HA) from microbial fermentation was purchased from Lifecore Biomedical (MN, USA) as sodium hyaluronate and used without further purification. CDDP was purchased from LC Laboratories (MA, USA). All other reagents were purchased from Fisher Scientific (PA, USA) or Sigma-Aldrich (MO, USA) and were of American Chemical Society (ACS) grade or better. Milli-Q water was used in all experiments. Human HNSCC cell line MDA-1986 was provided by Mark Cohen (University of Kansas Medical Center, KS, USA). Animal procedures were approved by the University of Kansas Institutional Animal Care and Use Committee. Athymic nude mice were purchased from Charles River Laboratories (MA, USA).

■ Synthesis of HA–Pt conjugates

Cisplatin was conjugated to HA (35,000 g/mol), based on the previously reported procedure [5]. Typically, HA (100 mg) and CDDP (45 mg) were dissolved in ddH_2O (20 ml) and stirred in the dark for 3 days at ambient temperature (~25°C). The mixture was filtered (0.2 µm nylon membrane) and dialyzed against ddH_2O (10,000 MWCO; Pierce, IL, USA) for 48 h at 4°C protected from light. Following dialysis, the crude product was concentrated and stored at 4°C. The degree of CDDP substitution was determined by atomic absorption spectroscopy (Varian SpectrAA GTA-110 with graphite furnace). The furnace program was as follows: ramp 25–80°C, hold 2 s, ramp to 120°C, hold 10 s, ramp to 1000°C, hold 5 s, ramp to 2700°C, hold 2 s, cool to 25°C over 20 s. The graphite partition tube was cleaned every 40 samples by baking at 2800°C for 7 s. Argon was used as the injection and carrier gas.

■ Cell toxicity

The HNSCC cell line MDA-1986 was maintained in Dulbecco's modified Eagle medium, supplemented with 10% fetal bovine serum and 1% L-glutamine–alanine. Preceding proliferation studies, cells were trypsinized and seeded into 96-well plates (5000 cells/well). After 24 h, CDDP, HA–Pt or HA was added (n = 12; seven concentrations) and 72 h post-addition, resazurin blue in 10 µl of phosphate-buffered saline was added to each well (final concentration of 5 µM). After 4 h, well fluorescence was measured (λ_{ex} 560 nm, λ_{em} 590 nm) using a fluorophotometer (SpectraMax Gemini; Molecular Devices, CA, USA). IC_{50} was determined as the midpoint between saline (positive) and cell-free (negative) controls for each plate.

■ Toxicology analysis

The hearing loss was measured in nude mice after three weekly doses of CDDP intravenous (i.v.) or HA–Pt subcutaneous (s.c.) chemotherapy. Saline was injected via the tail vein into a group of control animals. At the fourth week, a probe was placed inside the external auditory canal of anesthetized mice and an acoustic stimulus was delivered using Smart OAE (Intelligent Hearing Systems, FL, USA). Distortion product otoacoustic emission (DPOAE) was recorded and graphed. Frequencies tested range from 3000 to 32,000 Hz. Amplitude was recorded in dB SPL.

■ Pathology

Healthy nude mice were randomly divided into three groups and treated with HA–Pt s.c. (N = 3), CDDP i.v. (N = 3) or saline i.v. (N = 4) weekly at an equivalent dose (3.5 mg/kg). Animals were euthanized 2 weeks after the third treatment was completed. The liver, bilateral kidneys, brain, right (ipsilateral) and left (contralateral) axillary nodes and underlying tissue at the injection site were excised intact and stored in 80% alcoholic formalin solution overnight for fixation before slide mounting. Mounting using hematoxylin and eosin (H&E) staining were conducted by Veterinary Lab Resources (KS, USA). The pathological examination was performed by a blinded board-certified veterinarian pathologist (University of Kansas Medical Center).

■ Tumor model & *in vivo* imaging

The pCLNRX-turbo635 plasmid was constructed by inserting a 715-bp AfeI/HindIII fragment of the pTurboFP635C (Evrogen Inc, Moscow, Russia) into a 7675-bp AleI/HindIII fragment of the pCLNRX retrovirus-expression vector (Imgenex, CA, USA). The incorporation of the insert was verified by sequencing. Packaging 293-GPG cells were used to generate the retroviruses, followed by infecting MDA-1986 human HNSCC cells and selecting for 2 weeks with 0.8 mg/ml G418. Stable protein production and resulting strong cell near-infrared cell fluorescence was verified by fluorescence microscopy with a Texas Red filter (data not shown).

Stable MDA-1986/Turbo635 cells were prepared in 1 × PBS solution at a cell concentration of 10^7 cells/ml. 100 µl of the cell solution was injected under pentobarbital sedation into the oral mucosa layers of nude mice using 27-ga needles. Tumor size was measured twice a week by a digital caliper on mice anesthesized with 1.5–2% isoflurane in a 50% oxygen 50% ambient air mixture. Tumor volume was calculated using **Equation 1**.

$$Tumour\ volume\left(mm^3\right) = 0.52 \times \left(width\right)^2 \times length$$

Equation 1

Before imaging, mice were anesthetized, and HA–Texas Red (10 mg/ml in saline, 100 µl) was injected s.c. over the neck of the animal. The injection area was massaged gently for 5 min and fluorescently imaged over 24 h (CRI Maestro Flex, CRI Inc., MA, USA) using a 445–490 nm filtered halogen excitation light and a 515 nm longpass emission filter. Fluorescence was measured in 10 nm bandpass segments from 520 to 720 nm, using a cooled charge coupled device (CCD) camera with autoexposure. Images were spectrally unmixed using the automatic deconvolution tools (Maestro version 2.10) to limit skin and intestine autofluorescence resulting from chlorophyll in food.

■ Treatment

Female nude mice were injected with MDA-1986 cells and randomly divided into five groups: saline i.v. group (N = 5), HA s.c. group (N = 6), CDDP i.v. group (N = 5), HA–Pt s.c. group (N = 7), and HA–Pt i.v. group (N = 6). Animals in each group were euthanized once their tumor size reached 1000 mm^3 or 12 weeks after tumor cells were injected. In addition, animals were euthanized during the study if tumors ulcerated or infections unrelated to tumor growth occured. Facial tumors were observed 2 weeks after tumor cells were implanted. All treatments were administered 3, 4 and 5 weeks after tumor cell implantation. Three doses of 3.5 mg/kg CDDP, 3.5 mg/kg HA–Pt or physiological saline were administered i.v. via tail veins; or three doses of 3.5 mg/kg of HA–Pt or HA were administered s.c. around the tumors. The size of the primary tumor was measured weekly. A similar study was conducted using male nude mice, which were treated with either CDDP i.v. (N = 4, 3.5 mg/kg × 3 weeks) or HA–Pt s.c. (N = 4, equivalent dose on a platinum basis).

Results & discussion

■ Synthesis & *in vitro* toxicity of HA–Pt conjugates

Efficient conjugation between *cis*-diamminedichloroplatinum(II) and hyaluronic acid was reported in our previous studies with silver nitrate [6] or without silver nitrate as activating agent (data not shown). CDDP was successfully conjugated to the carboxylate group of hyaluronan (HA) with a substitution degree of approximately 25% w/w. HA–Pt nanoconjugates exhibited similar antiproliferative activity as the CDDP in human HNSCC cell line MDA-1986 (CDDP IC_{50} = 6.6 µM, HA–Pt IC_{50} = 6.0 µM) and human oral squamous cell cancer cell line JMAR (CDDP IC_{50} = 4.9 µM, HA–Pt IC_{50} = 6.1 µM). The *in vitro* toxicity of the conjugates was due to the toxicity of the slowly released active form of CDDP. Upon cleavage of the ester platinum bond, the released CDDP produces three forms of the hydrolyzed drug: the aqua form $(Pt[NH_3]_2[H_2O]_2)^{2+}$, the monohydroxo form $(Pt[NH_3]_2[H_2O][OH])^{+}$ and *di*hydroxo form $(Pt[NH_3]_2[OH]_2)$, which immediately redistribute to reach equilibrium. The active, monohydroxo form of the drug was determined to be the primary species at pH 6.0, based on the calculation using the first and second pK_a values for deprotonation (pK_{a1} 5.37 and pK_{a2} 7.21) [7]. The antiproliferative activity of HA–Pt conjugates is likely due to one or both of the following pathways, carrier-mediated endocytosis of HA–Pt conjugates, followed by the cleavage of the drug, or drug internalization via passive diffusion or active transport following the release of the drug. Conjugating multiple CDDP molecules to a HA molecule may change the mechanism of drug internalization from passive diffusion to carrier-mediated endocytosis over time, overcoming the likelihood of developing early drug resistance due to the presence of membrane efflux pumps.

Uptake of HA–Pt conjugates by MDA-1986 cells was confirmed using a fluorescently tagged HA conjugate, which was synthesized by condensation of Texas Red hydrazide to HA [6]. After 4 h incubation, uptake of HA–Texas Red into the cells was observed using an upright fluorescent microscope. The Texas red bound HA was widely distributed throughout the cytoplasm.

■ Toxicology analysis

Cisplatin is known to induce dose-dependent ototoxicity, leading to mostly irreversible auditory impairment, primarily in the high

frequencies, in both human and experimental animals [8,9]. CDDP is highly plasma-protein bound after i.v. administration. Approximately 96% of the drug becomes biologically inactive after it binds to the plasma protein, principally serum albumin; whereas the monohydrated fraction of the free drug causes ototoxicity and injuries to the cochlea [9,10]. CDDP ototoxicity is likely due to the generation and release of reactive oxygen species post-exposure of the mechanosensory hair cells to the active form of the drug [11]. Use of protective antioxidants was demonstrated to attenuate the injuries to the hair cells caused by CDDP chemotherapy due to a free radical scavenging effect [12–14].

In this study, mice in both control and treated groups (saline i.v., CDDP i.v. and HA–Pt s.c.) exhibited otoacoustic emission, which indicated that the CDDP-targeted mechanosensory hair cell in the inner ear region remained functional. However, no systemically significant differences were observed between groups, which is likely due to the relatively low doses (3.5 mg/kg × 3 weeks) that were administered. Zuur *et al.* reported that low-dose intravenous CDDP chemotherapy caused less acute hearing loss compared with high-dose therapy in a study of 60 patients [8]. Studies at a higher dose or more frequent dosing schedule may better reveal the influence of dosing to the degree of ototoxicity. In 2002, Chen *et al.* studied the maximum tolerated dose (MTD) of a CDDP-loaded biodegradable poly(D,L-lactide-co-glycolide) conjugate, and compared its MTD with the free unbound CDDP [15]. The results revealed that the polymer–drug conjugate had a MTD of 36 mg/kg, exhibiting a onefold increase relative to the free CDDP. Thus, an increased dose in our treatment regimen may be expected to induce a noticeable change in the ototoxicity.

Renal toxicity of CDDP is another dose-limiting side effect of the anticancer drug. In one of our previous studies, we examined the renal toxicity induced by the free CDDP (i.v., 1.0 and 3.3 mg/kg) or HA–Pt (s.c., formulation with or without silver, 1.0 and 3.3 mg/kg equivalent CDDP) [16]. The renal toxicity of the drug was monitored by the creatinine level in the urine of the Sprague–Dawley rats for up to 30 days following a single injection. The HA–Pt formulation with silver nitrate as an activating agent was eliminated from the study due to the renal toxicity it caused. The animals that were treated with either HA–Pt silver-free formulation or unbound CDDP did not demonstrate a statistically significant difference, which is due to the effective functional recovery of the rats following a single dose of the drug, as well as the relatively low dose that was administered. Therefore, we subsequently conducted a kidney pathological study to compare the extent of tissue degeneration and necrosis of their kidney sections. The results showed that the lymphatic HA–Pt formulation induced milder tissue damage and less renal dysfunction.

■ Pathology

At the conclusion of the 5-week toxicity study (weekly dose of 3.5 mg/kg for 3 weeks), animals were euthanized and a full pathological examination was performed. Kidney, liver, brain, lymph nodes and underlying tissue of the injection site were normal with no significant microscopic changes for all study groups. This is likely due to the low dosing level administered as well as the reduced drug uptake and accumulation or the upregulated tissue repair. Studies at a higher drug concentration, increased dosing frequency or reduced recovery time at the conclusion of the treatment may result in differentiated CDDP toxicities.

■ Tumor model & *in vivo* imaging

In this study, we established an orthotopic murine tumor model of HNSCC by injecting human HNSCC cells – MDA-1986 – into the buccal mucosa of nude mice. The model exhibited rapid and sustained tumor growth, with average survival of up to 12 weeks after tumor cell implantation. The primary tumor proceeded similarly to highly aggressive human HNSCC, invading the mandible and metastasizing to the cervical nodes. To validate the tumor model and verify the incidence of distant metastasis, we intactly removed the primary tumor and the draining lymph nodes from the animal and stored in formalin solution overnight for fixation before biopsies. H&E staining tests were conducted and the histology slides showed muscular (middle panel) and glandular (right panel) invasion of the cancer cells into the lymphatics **(Figure 1)**.

In order for our nanocarriers to deliver anticancer drugs to metastases in the head and neck locoregional lymphatics, carriers should drain from the tumor area to the diseased lymph nodes. We injected HA–Texas Red conjugates to evaluate the drainage into the diseased cervical lymph nodes 24 h post-injection **(Figure 2)**. The nanoconjugates slowly diffused from the

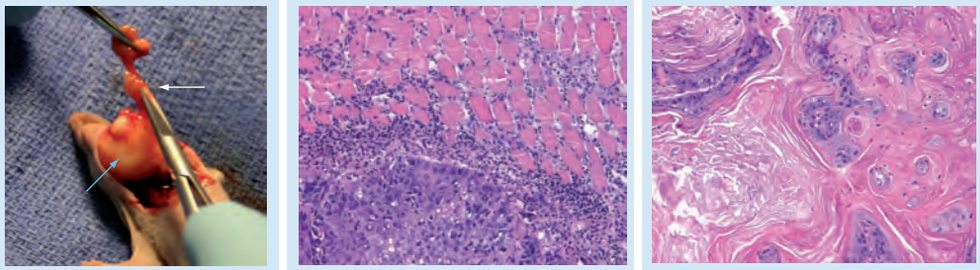

Figure 1. Orthotopic mouse model of head and neck squamous cell cancer showing primary tumor (bottom arrow) and lymphatic metastases (top arrow), and histology slides show muscular and glandular invasion.

Key Term

Mouse xenograft model: Tumor model that is established by inoculating human cancer cells into the tissue of mice that lack a functioning immune system.

injection site possibly to the primary tumor and peripheral locoregional lymphatics, which harbor the metastases. If the targeted drainage of the HA conjugates toward the neoplastic tissue occurred, it is likely to be due to the lymphangiogenesis, leading to the increased accumulation of the nanoconjugates adjacent to the tumor and the cervical lymph nodes. In order to verify the uptake, additional histological evidences for the targeted drainage using a fluorescent microscope will be conducted in our ongoing future experiments. Other polymeric carriers, such as optically labeled dendrimer [17] or dextran [18,19], have also been used to enable visualization of the lymphatic drainage.

In order to visualize tumor progression in the early stages, we developed a MDA-1986 cell line expressing red fluorescent protein. Initially the Turbo635 was inserted into the pLNCX2 vector (Clontech) under control of the CMV immediate early promoter with a neomycin insert and selected with G418. Although the resulting cells had strong fluorescence *in vitro*, tumor implants resulted in no fluorescence, leading us to believe that the promoter was shut off in this cell line after implantation. Replacement with the Hsp70 promoter resulted in strong expression of the fluorescent reporter gene *in vitro* and *in vivo*.

■ Treatment

Two groups of female nude mice treated with saline i.v. or HA s.c. developed tumors of approximately 1000 mm^3 on average after 5 weeks, which indicated that HA does not alter the natural progression of HNSCC. On the other hand, the female animals that were treated with three doses of either i.v. CDDP or i.v. HA–Pt developed tumors of approximately 1000 mm^3 8 weeks post-tumor cell implantation. By contrast, 57% of the female animals bearing HNSCC **xenografts** in the HA–Pt s.c. treated group (three equivalent doses of HA–Pt) were cured within 6 weeks with no disease recurrence by the end of the study **(Figure 3)**. In addition, survival rate was greatly improved for the animals treated with HA–Pt s.c. when compared with either of the control groups ($p = 0.0019$ for saline i.v. group and $p = 0.0027$ for HA s.c. group) or CDDP i.v. ($p = 0.0221$) and HA–Pt i.v. ($p = 0.0112$) groups using Gehan–Breslow–Wilcoxon rank analysis **(Figure 3)**. No statistically significant differences were observed for i.v.-treated CDDP and HA–Pt groups. Overall, the result of the tumor model suggests that HA–Pt conjugates achieved a higher anticancer efficacy relative to the conventional i.v. CDDP therapy due to the route of drug administration as well as the intrinsic properties of HA as a carrier for lymphatic drug delivery **(Figure 3)**. HA–Pt slowly released

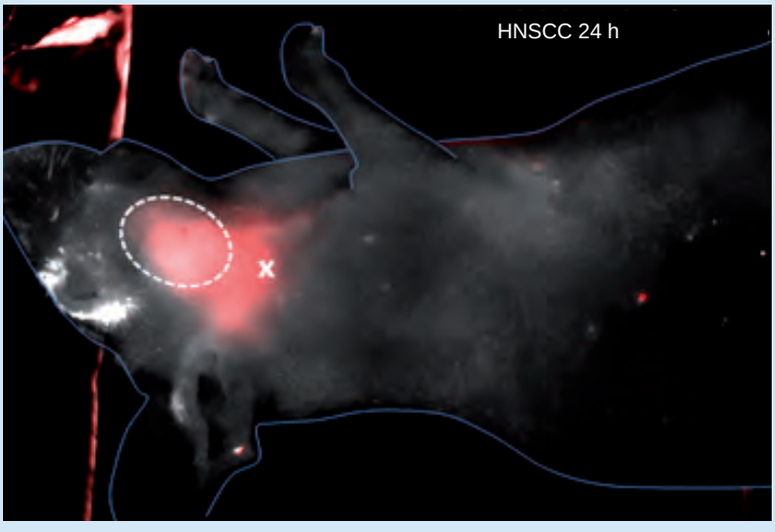

Figure 2. Hyaluronan–Texas red to the surrounding lymphatics (24 h post-injection). Dashed circle and × indicate the location of the primary tumor and the nearby injection site, respectively.
HNSCC: Head and neck squamous cell cancer.

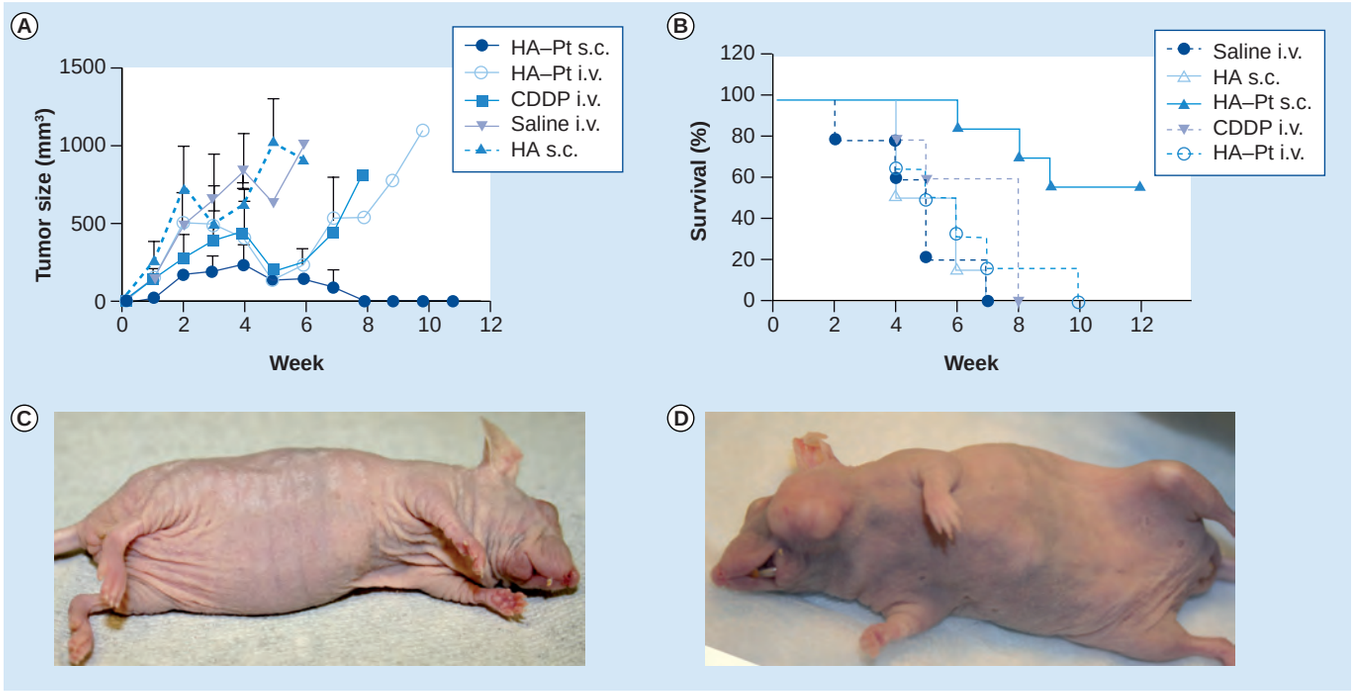

Figure 3. Measurement of tumor size. (A) Female animals were administered saline i.v., HA s.c., equivalent doses of CDDP i.v., HA–Pt s.c. and HA–Pt i.v. (3.5 mg/kg on Pt basis, 5 ≤ N ≤ 7). **(B)** Survival curves of female animals treated by saline, HA, CDDP or HA–Pt (5 ≤ N ≤ 7). **(C)** Lymphatic HA–Pt chemotherapy at 12 weeks. **(D)** Intravenous CDDP chemotherapy at 8 weeks.
CDDP: Cisplatin; HA: Hyaluronan; HA–Pt: Hyaluronan–cisplatin; i.v.: Intravenous; s.c.: Subcutaneous.

the active form of the drug, which subsequently drained to the adjacent cervical lymph nodes and the surrounding lymphatic regions. The gradually released CDDP did not cause any skin or tissue reaction at the injection site, even though CDDP is well known as a vesicant. This is likely due to the protective effect of HA, which has been used as a rescue medication to alleviate local toxicity effects of chemotherapeutics. A similar tumor suppression effect was also observed by Chen *et al.* in their treatment efficacy study using a CDDP-incorporated polymer conjugate against HNSCC in a chimeric mouse model [15]. Some effect may be due to the increased residence time of CDDP in plasma with the locally injected conjugates. However, this effect would be due to vascular uptake and subsequent extravasculation followed by lymphatic uptake in the head and neck region. In another study we recently published, levels in ipsilateral axilla nodes were compared with contralateral, and drug levels in the contralateral were similar to intravenous levels, with no local 'boost' in even these immediate-area lymphatics with a different drainage basin [16].

Administration of anticancer drugs via polymeric delivery vehicles is a promising method for local delivery of concentrated chemotherapeutics, effectively treating lymphatically metastatic cancers. A study by Dunne *et al.* revealed that CDDP-bound poly(ethylene oxide)-block-poly(lysine) block copolymer greatly hindered the tumor progression in a squamous cell carcinoma model of the upper aerodigestive tract in animals [20]. Another study carried out by Xie *et al.* reported an enhanced efficacy against laryngeal squamous cell carcinoma in rodents compared with conventional paclitaxel therapy [21].

Another interesting observation was that the tumor progression of HNSCC exhibited a more aggressive pattern in male nude mice compared with the female animals. All the male animals in the CDDP i.v. group reached an average tumor size of approximately 1000 mm^3 in 2 weeks **(Figure 4)** as opposed to 8 weeks, as observed in the previous female animal studies **(Figure 3)**. On the other hand, 80% of the male animals in the HA–Pt s.c. group developed tumors of approximately 1000 mm^3 in 3 weeks and 20% of the animals were able to live through the end of the fourth week **(Figure 4)**. Therefore, gender differences, as well as weight loss and stress, may be contributing factors that are responsible for the differentiated carcinoma progression. In addition, gender differences in the pharmacokinetics and tolerability of CDDP may also impact the differences in survival. Stakisaitis *et al.* found

in rats that CDDP-related hyponatermia and renal toxicity is more pronounced in males than females, although the mechanism is not understood [22]. In human studies, tobacco and alcohol consumption were believed to be the major, but not the only, factors inducing the occurrence and recurrence of HNSCC. Other factors, such as age, weight loss, nutritional status and complications may also play a role in the survival of patients [23]. Dahlstrom *et al.* conducted a demographic study of 172 never smoker–never drinker patients, describing the age and sex distribution of HNSCC patients, and identifying the specific types of most commonly diagnosed HNSCC [24]. A similar study was also performed by Onyango *et al.*, showing an overall male preponderance in the occurrence of HNSCC among 793 patience [25]. Additional factors affecting the disease progression and metastasis are still under investigation.

Conclusion

This study demonstrates that intralymphatic delivery of CDDP may be a promising treatment regimen to deliver chemotherapeutics to the primary malignancy, locoregional lymphatics and metastases, with greatly improved *in vivo* efficacy and survival compared with conventional CDDP chemotherapy. Successful completion of this study may provide a platform for the development of other polymeric drug-delivery models for the treatment of a wide spectrum of lymphatically metastatic cancers. The platinum-based HA conjugates can either be administered as a neoadjuvant therapy prior to surgery to reduce tumor size and control cancer progression, or given as an adjuvant therapy post-surgery to reduce the risk of recurrence and eradicate cancer residuals, such as micrometastases. In addition, due to the sustained release characteristics of the conjugate, weekly or biweekly HA–Pt injections could replace the conventional daily infusion, leading to improved patient compliance and reduced healthcare cost.

Future perspective

Despite major strides in cancer prevention and treatment during recent decades, there has been only a modest improvement in overall survival. Over half of HNSCC patients will face recurrence at some point, and these cancers recur because current imaging tools fail to detect occult disease or therapies fail to completely eradicate resistant disease. More frequent and intense radioimaging or stronger regimens of chemotherapy and radiation would be detrimental in the long run to patients' health and, therefore, new approaches are needed.

Localized therapies stand a stronger chance of eradicating residual disease since higher doses of chemotherapy can be administered without dose-limiting toxicity to the heart, kidneys and liver. Localized chemotherapy is already used to great success in the treament of peritoneal disease in colon cancer using heated intraperitoneal chemotherapy, limb melanomas with heated isolated limb perfusions and liver cancer using isolated limb perfusions. However, there is no way to isolate most organs and tissues for concentrated chemotherapy, such as the breasts, neck and lungs. For most tissues, the lymphatics are an ideal pathway for local therapy due to their importance in early cancer metastasis. Localized chemotherapy may become an important component

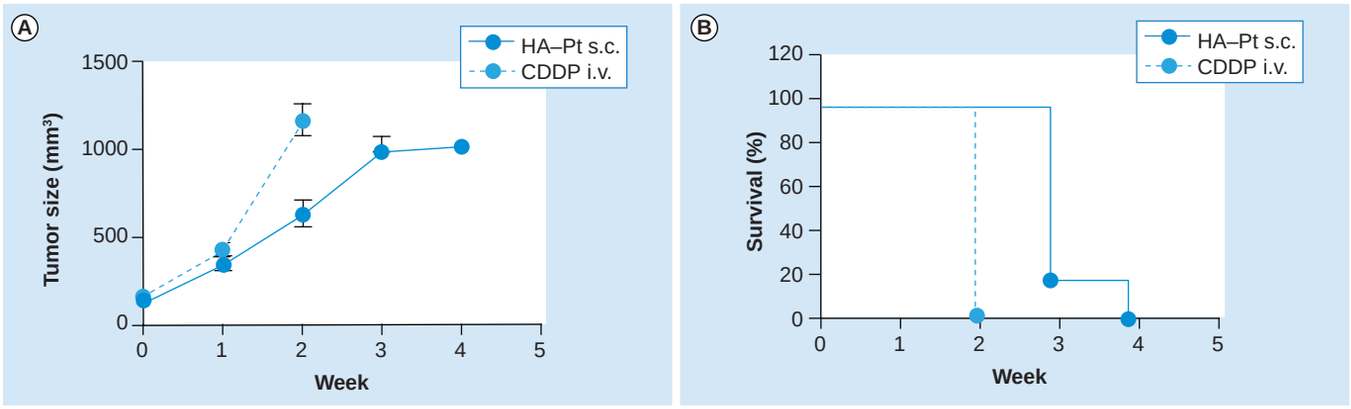

Figure 4. Measurements of tumor size and survival rate. (A) Tumor size and **(B)** survival rate. Male animals were administered equivalent doses of CDDP i.v. and HA–Pt s.c. (3.5 mg/kg on Pt basis, N = 4 for CDDP i.v., N = 6 for HA–Pt s.c.)
HA: Hyaluronan; HA–Pt: Hyaluronan–cisplatin; i.v.: Intravenous; s.c.: Subcutaneous.

in the treatment of early-stage cancers that are still confined to the primary tumor and local lymphatics; yet, to date, there are no tools in the clinic to localize chemotherapy in the lymph system.

Localized delivery systems such as we have described can effectively treat these early-stage diseases and we believe they will represent a new treatment option in the next 5–10 years. Next-generation systems will incorporate both imaging and diagnostic capabilities in the drug or drug carriers, so that the staging (or restaging) of the disease can be followed immediately by treatment to reduce treatment costs, limit the need for invasive surgeries and intravenous treatments and increase the likelihood that all disease can be eliminated in the early, more controllable stages.

Acknowledgements

Special thanks are given to David Pinson, DVM, (University of Kansas Medical Center, KS, USA) for valuable suggestions regarding the pathology studies.

Ethical conduct of research

The authors state that they have obtained appropriate institutional review board approval or have followed the principles outlined in the Declaration of Helsinki for all human or animal experimental investigations. In addition, for investigations involving human subjects, informed consent has been obtained from the participants involved.

Financial & competing interests disclosure

This work was supported by awards from the National Institutes of Health (R21 CA132033 to M Laird Forrest and P20 RR015563 subaward to M Laird Forrest) and the American Cancer Society (Research Scholar Grant RSG-08–133–01-CDD to M Laird Forrest). In addition, partial support for this project and its authors was provided by the University of Kansas General Research Fund and an Eli Lilly Predoctoral Fellowship (Shuang Cai). The authors have no other relevant affiliations or financial involvement with any organization or entity with a financial interest in or financial conflict with the subject matter or materials discussed in the manuscript apart from those disclosed.

No writing assistance was utilized in the production of this manuscript.

Executive summary

- Hyaluronan–cisplatin (HA–Pt) nanoconjugate was synthesized for the sustained release of cisplatin (CDDP).
- HA–Pt nanoconjugates exhibited similar antiproliferative activity as the CDDP in human head and neck squamous cell cancer (HNSCC) cell line MDA-1986.
- Uptake of HA–Pt conjugates by MDA-1986 cells was confirmed using a fluorescently tagged HA conjugate, HA–Texas Red, after incubation.
- No significant differences of CDDP-related ototoxicity were observed in nude mice that were treated with intravenous CDDP or subcutaneous HA–Pt due to the relatively low doses administered.
- Pathology study revealed that kidney, liver, brain, lymph nodes and underlying tissue of the injection site were normal with no significant microscopic changes for both intravenous CDDP and subcutaneous HA–Pt study groups.
- An orthotopic murine tumor model of HNSCC was established by injecting MDA-1986 cells into the buccal mucosa of nude mice. Hematoxylin and eosin staining tests and histology slides showed muscular and glandular invasion of the cancer cells into the lymphatics.
- HNSCC xenografts in the HA–Pt subcutaneous treated group (three equivalent doses of HA–Pt) were cured within 6 weeks with no disease recurrence by the end of the study.
- Survival rate was greatly improved for the animals treated with HA–Pt subcutaneous when compared with control groups ($p < 0.05$) or CDDP intravenous ($p < 0.05$) and HA–Pt intravenous ($p < 0.05$) groups.

Bibliography

Papers of special note have been highlighted as:
- ▪ of interest
- ▪▪ of considerable interest

1 Kurtin SE. Systemic therapies for squamous cell carcinoma of the head and neck. *Semin. Oncol. Nurs.* 25(3), 183–192 (2009).

▪▪ **Provides a discussion of current clinical therapies for the treatment of head and neck squamous cell carcinoma, emphasizing the balance between tumor response, drug-related toxicities and survival.**

2 Gil Z, Fliss DM. Contemporary management of head and neck cancers. *Isr. Med. Assoc. J.* 11(5), 296–300 (2009).

3 Forastiere AA. Chemotherapy in the treatment of locally advanced head and neck cancer. *J. Surg. Oncol.* 97(8), 701–707 (2008).

4 Chandana SR, Conley BA. Neoadjuvant chemotherapy for locally advanced squamous cancers of the head and neck: current status and future prospects. *Curr. Opin. Oncol.* 21(3), 218–223 (2009).

5 Jeong YI, Kim ST, Jin SG *et al.* Cisplatin-incorporated hyaluronic acid nanoparticles based on ion-complex formation. *J. Pharm. Sci.* 97(3), 1268–1276 (2008).

6 Cai S, Xie Y, Bagby T, Cohen MS, Forrest ML. Intralymphatic chemotherapy using a hyaluronan-cisplatin conjugate. *J. Surg. Res.* 147(2), 247–252 (2008).

▪▪ **Provides a general overview of breast cancer spread in the lymphatics and demonstrates an intralymphatic drug-delivery method in breast cancer.**

7 Pereira-Maia E, Garnier-Suillerot A. Impaired hydrolysis of cisplatin derivatives to aquated species prevents energy-dependent uptake in glc4 cells resistant to cisplatin. *J. Biol. Inorg. Chem.* 8(6), 626–634 (2003).

8 Zuur CL, Simis YJ, Verkaik RS *et al.* Hearing loss due to concurrent daily low-dose cisplatin chemoradiation for locally advanced head and neck cancer. *Radiother. Oncol.* 89(1), 38–43 (2008).

9 Ekborn A, Lindberg A, Laurell G, Wallin I, Eksborg S, Ehrsson H. Ototoxicity, nephrotoxicity and pharmacokinetics of cisplatin and its monohydrated complex in the guinea pig. *Cancer Chemother. Pharmacol.* 51(1), 36–42 (2003).

10 Vreeburg GC, Stell PM, Holding JD, Lindup WE. Cisplatin–albumin complex for treatment of cancer of the head and neck. *J. Laryngol. Otol.* 106(9), 832–833 (1992).

11 Clerici WJ, Hensley K, Dimartino DL, Butterfield DA. Direct detection of ototoxicant-induced reactive oxygen species generation in cochlear explants. *Hear. Res.* 98(1–2), 116–124 (1996).

▪ **Discusses the relationship between ototoxicity and the formation of reactive oxygen species.**

12 Huang X, Whitworth CA, Rybak LP. Ginkgo biloba extract (egb 761) protects against cisplatin-induced ototoxicity in rats. *Otol. Neurotol.* 28(6), 828–833 (2007).

13 Campbell KC, Meech RP, Klemens JJ *et al.* Prevention of noise- and drug-induced hearing loss with D-methionine. *Hear. Res.* 226(1–2), 92–103 (2007).

14 Kalcioglu MT, Kizilay A, Gulec M *et al.* The protective effect of erdosteine against ototoxicity induced by cisplatin in rats. *Eur. Arch. Otorhinolaryngol.* 262(10), 856–863 (2005).

15 Chen FA, Kuriakose MA, Zhou MX, Delacure MD, Dunn RL. Biodegradable polymer-mediated intratumoral delivery of cisplatin for treatment of human head and neck squamous cell carcinoma in a chimeric mouse model. *Head Neck* 25(7), 554–560 (2003).

16 Cai S, Xie Y, Davies NM, Cohen MS, Forrest ML. Pharmacokinetics and disposition of a localized lymphatic polymeric hyaluronan conjugate of cisplatin in rodents. *J. Pharm. Sci.* 99(6), 2664–2671 (2010).

17 Kobayashi H, Ogawa M, Kosaka N, Choyke PL, Urano Y. Multicolor imaging of lymphatic function with two nanomaterials: quantum dot-labeled cancer cells and dendrimer-based optical agents. *Nanomedicine* 4(4), 411–419 (2009).

▪ **Provides an overview of lymphatic imaging using quantum dot-labeled cancer cells and dendrimer-based agents to assist the diagnosis of metastatic sentinel lymph node.**

18 Vieira SC, Sousa RB, Tavares MB *et al.* Preoperative pelvic lymphoscintigraphy is of limited usefulness for sentinel lymph node detection in cervical cancer. *Eur. J. Obstet. Gynecol. Reprod. Biol.* 145(1), 96–99 (2009).

19 McElroy M, Bouvet M, Hoffman RM. Chapter 2. Color-coded fluorescent mouse models of cancer cell interactions with blood vessels and lymphatics. *Methods Enzymol.* 445, 27–52 (2008).

20 Dunne AA, Boerner HG, Kukula H *et al.* Block copolymer carrier systems for translymphatic chemotherapy of lymph node metastases. *Anticancer Res.* 27(6B), 3935–3940 (2007).

21 Xie M, Zhou L, Hu T, Yao M. Intratumoral delivery of paclitaxel-loaded poly(lactic-co-glycolic acid) microspheres for Hep-2 laryngeal squamous cell carcinoma xenografts. *Anticancer Drugs* 18(4), 459–466 (2007).

22 Stakisaitis D, Dudeniene G, Jankunas RJ, Grazeliene G, Didziapetriene J, Pundziene B. Cisplatin increases urinary sodium excretion in rats: gender-related differences. *Medicina (Kaunas)* 46(1), 45–50 (2010).

23 Van Bokhorst-De Van Der Schueren MAE, Van Leeuwen PA, Kuik DJ *et al.* The impact of nutritional status on the prognoses of patients with advanced head and neck cancer. *Cancer* 86(3), 519–527 (1999).

24 Dahlstrom KR, Little JA, Zafereo ME, Lung M, Wei Q, Sturgis EM. Squamous cell carcinoma of the head and neck in never smoker-never drinkers: a descriptive epidemiologic study. *Head Neck* 30(1), 75–84 (2008).

25 Onyango JF, Awange DO, Njiru A, Macharia IM. Pattern of occurrence of head and neck cancer presenting at Kenyatta National Hospital, Nairobi. *East Afr. Med. J.* 83(5), 288–291 (2006).